Available online at www.sciencedirect.com
ScienceDirect
European Journal of Mechanics B/Fluids 26 (2007) 182–192

A linearization of Mieussens's discrete velocity model for kinetic equations

Yingsong Zheng [a], Henning Struchtrup [b,*]

[a] *Department of Mechanical Engineering, University of Strathclyde, Glasgow, G1 1XJ, UK*
[b] *Department of Mechanical Engineering, University of Victoria, Victoria, V8W 3P6, Canada*

Received 14 September 2005; received in revised form 23 March 2006; accepted 31 August 2006

Available online 28 September 2006

Abstract

A linearization is developed for Mieussens's discrete velocity model (see, e.g., [L. Mieussens, Discrete-velocity models and numerical schemes for the Boltzmann-BGK equation in plane and axisymmetric geometries, J. Comput. Phys. 162 (2000) 429–466]) for kinetic equations. The basic idea is to use a linearized expression of the reference distribution function in the kinetic equation, instead of its exact expression, in the numerical scheme. This modified scheme is applied to various kinetic models, which include the BGK model, the ES-BGK model, the BGK model with velocity-dependent collision frequency, and the recently proposed ES-BGK model with velocity-dependent collision frequency. One-dimensional stationary shock waves and stationary planar Couette flow, which are two benchmark problems for rarefied gas flows, are chosen as test examples. Molecules are modeled as Maxwell molecules and hard sphere molecules. It is found that results from the modified scheme are very similar to results from the original Mieussens's numerical scheme for various kinetic equations in almost all tests we did, while, depending on the test case, 20–40 percent of computational time can be saved. The application of the method is not affected by the Knudsen number and molecular models, but is restricted to lower Mach numbers for the BGK (or the ES-BGK) model with velocity-dependent collision frequency.

Keywords: Rarefied gas dynamics; Kinetic equation; Discrete velocity model; Shock waves; Couette flow

1. Introduction

The Boltzmann equation, which is the fundamental equation of rarefied gas dynamics, is a nonlinear integro-differential equation, and difficult to handle. Therefore, kinetic models have been proposed with simplified expressions for the collision term in the Boltzmann equation [1–5].

Discrete Velocity Models (DVMs) offer a deterministic approach to the approximate solution of the Boltzmann equation with kinetic models [2,3]. Among the existing DVMs, Mieussens's DVM [5–10] is particularly interesting, since the distribution function remains always positive, and conservation laws and dissipation of entropy are ensured at the discrete level. Moreover, computational time can be saved from Mieussens's DVM, compared to traditional DVMs, since the number of discrete velocities does not need to be too large. These features are achieved since the

* Corresponding author. Tel.: +1 250 721 8916; fax: +1 250 721 6051.
E-mail addresses: ys_zheng@hotmail.com (Y. Zheng), struchtr@me.uvic.ca (H. Struchtrup).

0997-7546/$ – see front matter
doi:10.1016/j.euromechflu.2006.08.003

reference distribution functions f_{ref} in the kinetic models are not discretized directly, but determined by the discrete minimum entropy principle [6,7]. This numerical method has been applied successfully to the BGK model, the ES-BGK model, the BGK model with Velocity-Dependent Collision Frequency (VDCF) ($\nu(C)$-BGK model), and the ES-BGK model with VDCF ($\nu(C)$-ES-BGK model) [5–10].

In order to save computational time, and reduce the complexity of the program code further, Mieussens's original DVM is simplified in this paper by using a linearized expression of the reference distribution in the kinetic equation, instead of its exact expression.

Numerical tests are performed for one dimensional shock waves at steady state and planar Couette flow at steady state, which are two important benchmark problems for rarefied gas flows. Molecules are modeled as Maxwell molecules and hard sphere molecules [1].

2. Kinetic models and kinetic equations

In the microscopic theory of rarefied gas dynamics, the state variable is the (mass) distribution function $f(x_i, c_i, t)$, which specifies the density of microscopic particles with velocity c_i at time t and position x_i. The particles, which can be thought of as idealized atoms, move freely in space unless they undergo collisions. The corresponding evolution of f is described by the Boltzmann equation [1–4], which, when external forces are omitted, is written as

$$\frac{\partial f}{\partial t} + c_i \frac{\partial f}{\partial x_i} = S(f). \tag{1}$$

Here, the term on the right-hand side, $S(f)$, describes the change of f due to collisions among particles.

In the macroscopic continuum theory of rarefied gas dynamics, the state of the gas is described by macroscopic variables, such as mass density ρ, macroscopic flow velocity u_i, temperature T, and so on, which depend on position x_i and time t. These quantities can be recovered from the distribution f by taking velocity averages (or say, moments) of the corresponding microscopic quantities:

$$\begin{aligned}
&\rho = \int f \,\mathrm{d}c_1\,\mathrm{d}c_2\,\mathrm{d}c_3 = \int f \,\mathrm{d}\mathbf{c}, \qquad \rho u_i = \int c_i f \,\mathrm{d}\mathbf{c},\\
&p = \rho RT = \frac{1}{3}\int C^2 f \,\mathrm{d}\mathbf{c}, \qquad p_{ij} = \int f C_i C_j \,\mathrm{d}\mathbf{c} = p\delta_{ij} + \sigma_{ij},\\
&\sigma_{ij} = \int f C_{<i} C_{j>} \,\mathrm{d}\mathbf{c}, \qquad q_i = \frac{1}{2}\int C^2 C_i f \,\mathrm{d}\mathbf{c}.
\end{aligned} \tag{2}$$

Here $R = k/m$ is the gas constant, m is the mass of one microscopic particle, k is the Boltzmann constant, $C_i = c_i - u_i$ is the peculiar velocity, p is the hydrostatic pressure, p_{ij} is the pressure tensor, δ_{ij} is the unit matrix, q_i is the heat flux, and σ_{ij} is the trace-free part of the pressure tensor. An angular bracket around indices denotes the symmetric and trace-free part of a tensor, i.e. $C_{<i}C_{j>} = C_i C_j - C^2\delta_{ij}/3$. For more details on the computation of symmetric and trace-free tensors, please refer to [1]. The third expression in Eqs. (2) gives the definition of temperature for the ideal gas law.

In kinetic models, the Boltzmann collision term $S(f)$ is replaced by a relaxation expression which is typically of the form

$$S_m(f) = -\nu_{\text{ref}}(f - f_{\text{ref}}). \tag{3}$$

Here, f_{ref} is a suitable reference distribution function, and ν_{ref} is the collision frequency. The subscript ref will be replaced by the name of the kinetic model, when a specific kinetic model is applied. The various kinetic models differ in their choices of reference distribution f_{ref} and collision frequency ν_{ref} [5,10], while all kinetic models need to guarantee the conservation laws for mass, momentum and energy, which read

$$\int S_m \,\mathrm{d}\mathbf{c} = 0, \quad \int c_i S_m \,\mathrm{d}\mathbf{c} = 0, \quad \frac{1}{2}\int c^2 S_m \,\mathrm{d}\mathbf{c} = 0. \tag{4}$$

Several kinetic models have been proposed in the literature. Here, only the reference distributions of those kinetic models, which relate to this work, will be given. For more detailed information about these and other kinetic models please refer to [5,10].

The BGK model [1,3,11] is the original and simplest kinetic model; its reference distribution is simply the Maxwellian distribution,

$$f_{\text{ref}} = f_{\text{BGK}} = \rho\sqrt{\left(\frac{1}{2\pi RT}\right)^3}\exp\left(-\frac{C^2}{2RT}\right), \tag{5}$$

where the subscript BGK denotes a quantity used in the BGK model. ν_{BGK} depends on density and temperature, but is independent of the microscopic velocity.

The ES-BGK model [1,12–14] replaces the Maxwellian with a generalized Gaussian, so that

$$f_{\text{ref}} = f_{\text{ES}} = \rho\big(\det(2\pi\lambda_{ij})\big)^{-1/2}\exp\left(-\frac{1}{2}C_i\varepsilon_{ij}C_j\right), \tag{6}$$

where the subscript ES denotes a quantity used in the ES-BGK model. ν_{ES} depends on density and temperature, but is independent of the microscopic velocity.

The matrix λ_{ij} is given by

$$\lambda_{ij} = RT\delta_{ij} + b\sigma_{ij}/\rho = (1-b)RT\delta_{ij} + bp_{ij}/\rho, \tag{7}$$

where b is a number that serves to adjust the Prandtl number, and ε_{ij} is the inverse of the tensor λ_{ij}. The parameter b must lie in the interval $[-1/2, 1]$ to ensure that λ_{ij} is positive definite, which further ensures the integrability of f_{ES}. In the ES-BGK model, the reference distribution f_{ES} is in fact defined by the following ten conditions (the first five conditions are the conservation laws, Eqs. (4)),

$$\int f_{\text{ES}}\,\mathrm{d}\mathbf{c} = \rho, \quad \int C_i f_{\text{ES}}\,\mathrm{d}\mathbf{c} = 0, \quad \int C_iC_j f_{\text{ES}}\,\mathrm{d}\mathbf{c} = \rho\lambda_{ij} = (1-b)p\delta_{ij} + bp_{ij}, \tag{8}$$

which will be used in the numerical work later.

The $\nu(C)$-BGK model [9,10,15–18] (or say, the BGK model with VDCF) is an extension of the classical BGK model that allows incorporating the VCDF. The corresponding reference distribution in this kinetic model is a shifted Maxwellian,

$$f_{\text{ref}} = f_\gamma = a\exp\big(-\Gamma C^2 + \gamma_i C_i\big), \tag{9}$$

where the subscript γ denotes a quantity used in the $\nu(C)$-BGK model, and the coefficients a, Γ, and γ_i are chosen so as to guarantee the conservation of mass, momentum and energy as given in Eqs. (4). ν_γ depends on density and temperature, and also depends on the microscopic velocity [9,10].

In the $\nu(C)$-ES-BGK model [5,10,19], or say the ES-BGK model with VDCF, the reference distribution is written as

$$f_{\text{ref}} = f_N = a\exp\left(-\frac{1}{2}\Gamma\varepsilon_{ij}C_iC_j + \gamma_iC_i\right), \tag{10}$$

where the subscript N denotes a quantity used in the $\nu(C)$-ES-BGK model. Here, the matrix ε_{ij} has the same expression as in the ES-BGK model. The coefficients a, Γ, and γ_i are chosen so as to guarantee the conservation of mass, momentum and energy. ν_N depends on density and temperature, and also depends on the microscopic velocity [10].

3. Mieussens's discrete velocity model for kinetic equations

For one-dimensional shock waves, flow is along the x direction in an $x-y-z$ Cartesian frame. In the planar Couette flow problem, there are two parallel infinite plates in the $y-z$ plane (one plate is fixed, while the other plate is moving with a certain speed in the y direction), and the direction perpendicular to the plates is the x direction. The flow in the planar Couette flow is along the y direction. Therefore, macroscopic variables in both stationary situations vary only in the x direction.

The numerical method we use is based on the explicit scheme of Mieussens's DVM. Here, since its modification is the main aim of this paper, we shall only discuss the discrete reference distribution to save space. Other important details related to the numerical scheme, in particular the choice of boundary conditions, time step, space grid and velocity grid, can be found in Refs. [5–10].

In the following, a dense notation is used, e.g.

$$f\left(x_i, t_n, c_x^{j_1}, c_y^{j_2}, c_z^{j_3}\right) = f^n_{i,j_1,j_2,j_3} = f^n_{i,j}, \tag{11}$$

where x_i is the discrete space node in the x direction, t_n is the time after n time steps. Therefore, in Sections 3 and 4, a superscript n denotes values after n time steps, a subscript i denotes values at position x_i, and a subscript j denotes values at the discrete velocity node (j_1, j_2, j_3). Then, the discretized kinetic equation based on an explicit finite volume scheme is

$$f^{n+1}_{i,j} = f^n_{i,j} - \frac{\Delta t_n}{\Delta x}\left(F^n_{i+\frac{1}{2},j} - F^n_{i-\frac{1}{2},j}\right) - \Delta t_n \nu^n_{i,j}\left(f^n_{i,j} - f^n_{\mathrm{ref},i,j}\right), \tag{12}$$

where Δt_n is the nth time step, $\nu^n_{i,j}$ is the discrete collision frequency, Δx is the step size of the position grid, and $F^n_{i\pm\frac{1}{2},j}$ are the numerical fluxes [6,10,20]. As in Section 2, the subscript ref will be replaced by the name of the kinetic model, when a specific kinetic model is applied. We are interested in steady state solutions which are obtained by applying an iterative technique.

The main feature of Mieussens's DVM is that the coefficients in the reference distribution functions f_{ref} are not discretized directly, but determined by the discrete minimum entropy principle [6–8]. This is equivalent to obtaining the coefficients in the reference distribution from the discrete constraints of the reference distribution (e.g. Eqs. (16) below for the BGK model).

Obviously, the values of the coefficients in the discrete reference distributions are not identical to their values in the continuous situation. In fact, if we choose the values of the coefficients directly from the continuous case (by setting $\gamma^n_{\mathrm{BGK},i} = 0$ in the following Eq. (14) for the BGK model), which was called the "natural approximation" by Mieussens [6,7], the conservation laws and dissipation of entropy will not be strictly satisfied in the discrete case [6,7]. We emphasize that in the continuum limit, where the bounds of the discrete velocity approach infinity, and the step sizes of the velocity grid approach zero, Mieussens's DVM will be equivalent to DVMs where the natural approximation is applied [8].

Since a nonlinear system of equations is easier and more robust to be solved when the magnitudes of the terms in all equations are similar, dimensionless quantities are used in the code. The discrete dimensionless reference distribution $F^n_{\mathrm{ref},i,j}$ is defined by

$$f^n_{\mathrm{ref},i,j} = F^n_{\mathrm{ref},i,j}\frac{\rho^n_i}{\Delta\mathbf{c}}, \tag{13}$$

where $\Delta\mathbf{c}$ denotes the volume of a cell in discrete velocity space.

For the BGK model in the shock waves, the dimensionless reference distribution reads

$$F^n_{\mathrm{BGK},i,j} = \frac{f^n_{\mathrm{BGK},i,j}\Delta\mathbf{c}}{\rho^n_i} = a^n_{\mathrm{BGK},i}\exp\left(-\Gamma^n_{\mathrm{BGK},i}\left(\eta^n_{i,j}\right)^2 + \gamma^n_{\mathrm{BGK},i}\eta^n_{i,j_1}\right), \tag{14}$$

where

$$\eta^n_{i,j} = C_j/\sqrt{2RT^n_i} \tag{15}$$

is the dimensionless peculiar velocity, and $(\eta^n_{i,j})^2 = (\eta^n_{i,j_1})^2 + (\eta^n_{i,j_2})^2 + (\eta^n_{i,j_3})^2$. The dimensionless coefficients $a^n_{\mathrm{BGK},i}$, $\Gamma^n_{\mathrm{BGK},i}$ and $\gamma^n_{\mathrm{BGK},i}$ must be determined from the conservation laws, Eqs. (4), which in the discrete case read

$$\sum_{j=1}^{J} F^n_{\mathrm{BGK},i,j} = 1, \quad \sum_{j=1}^{J}\eta^n_{i,j_1}F^n_{\mathrm{BGK},i,j} = 0, \quad \sum_{j=1}^{J}\frac{(\eta^n_{i,j})^2}{1.5}F^n_{\mathrm{BGK},i,j} = 1. \tag{16}$$

By inserting the dimensionless distribution (14) into Eqs. (16), we obtain the final system of equations to determine the three coefficients as

$$\sum_{j=1}^{J} a^n_{\mathrm{BGK},i}\exp\left(-\Gamma^n_{\mathrm{BGK},i}\left(\eta^n_{i,j}\right)^2 + \gamma^n_{\mathrm{BGK},i}\eta^n_{i,j_1}\right) = 1,$$

$$\sum_{j=1}^{J} \eta_{i,j_1}^n a_{\mathrm{BGK},i}^n \exp\bigl(-\Gamma_{\mathrm{BGK},i}^n \bigl(\eta_{i,j}^n\bigr)^2 + \gamma_{\mathrm{BGK},i}^n \eta_{i,j_1}^n\bigr) = 0, \tag{17}$$

$$\sum_{j=1}^{J} \bigl(\eta_{i,j}^n\bigr)^2 a_{\mathrm{BGK},i}^n \exp\bigl(-\Gamma_{\mathrm{BGK},i}^n \bigl(\eta_{i,j}^n\bigr)^2 + \gamma_{\mathrm{BGK},i}^n \eta_{i,j_1}^n\bigr) = 1.5,$$

which is obviously a nonlinear system of equations for unknown coefficients $a_{\mathrm{BGK},i}^n$, $\Gamma_{\mathrm{BGK},i}^n$, $\gamma_{\mathrm{BGK},i}^n$. This nonlinear system must be solved at each position node and for every time step. The Newton–Raphson (N–R) algorithm [21] (also known as the Newton method with a backtracking line search [22]) is applied to solve the nonlinear system in our work here as well as in Refs. [5,10] and in Mieussens's work [6–9].

For the ES-BGK model in the shock waves, the dimensionless reference distribution is

$$F_{\mathrm{ES},i,j}^n = a_{\mathrm{ES},i}^n \exp\bigl(-\Gamma_{\mathrm{ES},xx,i}^n \bigl(\eta_{i,j_1}^n\bigr)^2 - \Gamma_{\mathrm{ES},yy,i}^n \bigl(\bigl(\eta_{i,j_2}^n\bigr)^2 + \bigl(\eta_{i,j_3}^n\bigr)^2\bigr) + \gamma_{\mathrm{ES},i}^n \eta_{i,j_1}^n\bigr), \tag{18}$$

and the conditions [6,23] to determine the four coefficients are the discrete form of Eqs. (8).

Expressions for $F_{\mathrm{ref},i,j}^n$ and discrete constraints for kinetic models in other flow situations can be built following the same ideas as above [5,10].

4. A linearization of Mieussens's discrete velocity model

As we see from the above Section 3, the equations to determine coefficients in the discrete reference distribution $f_{\mathrm{ref},i,j}^n$ form a nonlinear system of equations, and the N–R algorithm (or another nonlinear solver) is needed to solve the equations. This makes the program code complex and requires a considerable amount of computational time.

Note that the reference distribution for the continuous BGK model is the local Maxwellian, Eq. (5). Thus, as was shown by Mieussens in [8], in the continuous limit (infinitely many velocity nodes) the coefficients in the discrete dimensionless reference distribution expression (14) assume the values $a_{\mathrm{BGK},i}^n = \Delta\mathbf{c}/\sqrt{(2\pi R T_i^n)^3}$, $\Gamma_{\mathrm{BGK},i}^n = 1$, and $\gamma_{\mathrm{BGK},i}^n = 0$. For a reasonably fine velocity grid the coefficients will differ only slightly from these values, which allows a linearization of the scheme.

Therefore, in order to simplify the program and save computational time, and simultaneously obtain the same results, we propose to use a linearized discrete reference distribution $f_{\mathrm{ref},i,j}^n$, instead of the original nonlinear distribution. Then the system of equations for the undetermined coefficients becomes a linear system, which can be solved much faster and easier.

For the BGK model and the $\nu(C)$-BGK model, in which an isotropic Gaussian distribution appears in the original reference distribution, the way to construct the linearization is to expand the original reference distribution around the Maxwellian distribution, which is an isotropic Gaussian distribution. Following this idea, we obtain the linearized dimensionless reference distribution in the BGK model for the shock waves as

$$F_{\mathrm{BGK},i,j}^n = \exp\bigl(-\bigl(\eta_{i,j}^n\bigr)^2\bigr)\bigl(a1_{\mathrm{BGK},i}^n + a2_{\mathrm{BGK},i}^n \eta_{i,j_1}^n + a3_{\mathrm{BGK},i}^n \bigl(\eta_{i,j}^n\bigr)^2\bigr), \tag{19}$$

and now $a1_{\mathrm{BGK},i}^n$, $a2_{\mathrm{BGK},i}^n$, $a3_{\mathrm{BGK},i}^n$ are the three undetermined (dimensionless) coefficients. Within the validity of the linearization, the relation between new and old coefficients is given by

$$a1_{\mathrm{BGK},i}^n = a_{\mathrm{BGK},i}^n, \quad a2_{\mathrm{BGK},i}^n \cong a_{\mathrm{BGK},i}^n \gamma_{\mathrm{BGK},i}^n, \quad a3_{\mathrm{BGK},i}^n \cong -a_{\mathrm{BGK},i}^n \bigl(\Gamma_{\mathrm{BGK},i}^n - 1\bigr). \tag{20}$$

Note that for the exact BGK model the coefficients $a2_{\mathrm{BGK},i}^n$ and $a3_{\mathrm{BGK},i}^n$ vanish. Since Mieussens's scheme converges to the BGK equation for increasing number of discrete velocities [8], the coefficients $\gamma_{\mathrm{BGK},i}^n$ and $(\Gamma_{\mathrm{BGK},i}^n - 1)$ are small, which allows Taylor expansion in these coefficients. The Taylor expansion leads to our linearized scheme.

The essential constraints for these three unknown coefficients are still the conservation laws Eqs. (16). Insertion of the expression (19) into Eqs. (16) gives the system of equations for the new coefficients as

$$\begin{aligned}
&a1_{\mathrm{BGK},i}^n J_{i,11}^n + a2_{\mathrm{BGK},i}^n J_{i,12}^n + a3_{\mathrm{BGK},i}^n J_{i,13}^n = 1,\\
&a1_{\mathrm{BGK},i}^n J_{i,21}^n + a2_{\mathrm{BGK},i}^n J_{i,22}^n + a3_{\mathrm{BGK},i}^n J_{i,23}^n = 0,\\
&a1_{\mathrm{BGK},i}^n J_{i,31}^n + a2_{\mathrm{BGK},i}^n J_{i,32}^n + a3_{\mathrm{BGK},i}^n J_{i,33}^n = 1.5,
\end{aligned} \tag{21}$$

where

$$\mathbf{J}_i^n = \begin{bmatrix} \sum_{j=1}^J \exp(-(\eta_{i,j}^n)^2) & \sum_{j=1}^J \eta_{i,j_1}^n \exp(-(\eta_{i,j}^n)^2) & \sum_{j=1}^J (\eta_{i,j}^n)^2 \exp(-(\eta_{i,j}^n)^2) \\ \sum_{j=1}^J \eta_{i,j_1}^n \exp(-(\eta_{i,j}^n)^2) & \sum_{j=1}^J (\eta_{i,j_1}^n)^2 \exp(-(\eta_{i,j}^n)^2) & \sum_{j=1}^J (\eta_{i,j}^n)^2 \eta_{i,j_1}^n \exp(-(\eta_{i,j}^n)^2) \\ \sum_{j=1}^J (\eta_{i,j}^n)^2 \exp(-(\eta_{i,j}^n)^2) & \sum_{j=1}^J \eta_{i,j_1}^n (\eta_{i,j}^n)^2 \exp(-(\eta_{i,j}^n)^2) & \sum_{j=1}^J (\eta_{i,j}^n)^2 (\eta_{i,j}^n)^2 \exp(-(\eta_{i,j}^n)^2) \end{bmatrix},$$

which is a symmetric matrix. The above linear system of equations for $a1_{\mathrm{BGK},i}^n$, $a2_{\mathrm{BGK},i}^n$, and $a3_{\mathrm{BGK},i}^n$ can be solved faster than the original nonlinear system of equations for $a_{\mathrm{BGK},i}^n$, $\Gamma_{\mathrm{BGK},i}^n$ and $\gamma_{\mathrm{BGK},i}^n$ (Eqs. (17)). Since the system must be solved for each position node at every time step, a noticeable reduction of the computational time can be expected.

For the ES-BGK model and the $\nu(C)$-ES-BGK model, in which an anisotropic Gaussian distribution appears in the original reference distribution, we construct the linearization by expanding their original reference distribution around a suitable anisotropic Gaussian distribution. This gives the linearized reference distribution in the ES-BGK model for the shock waves as

$$\begin{aligned} F_{\mathrm{ES},i,j}^n = {} & \exp\bigl(-\varepsilon_{\mathrm{ES},xx,i}^n \bigl(\eta_{i,j_1}^n\bigr)^2 - \varepsilon_{\mathrm{ES},yy,i}^n \bigl(\bigl(\eta_{i,j_2}^n\bigr)^2 + \bigl(\eta_{i,j_3}^n\bigr)^2\bigr)\bigr) \\ & \times \bigl(a1_{\mathrm{ES},i}^n + a2_{\mathrm{ES},i}^n \eta_{i,j_1}^n + a3_{\mathrm{ES},i}^n \bigl(\eta_{i,j_1}^n\bigr)^2 + a4_{\mathrm{ES},i}^n \bigl(\bigl(\eta_{i,j_2}^n\bigr)^2 + \bigl(\eta_{i,j_3}^n\bigr)^2\bigr)\bigr). \end{aligned} \tag{22}$$

Here

$$\varepsilon_{\mathrm{ES},xx,i}^n = \frac{p_i^n}{p_{\mathrm{BGK},xx,i}^n/Pr + (1-1/Pr)p_{xx,i}^n} \quad \text{and} \quad \varepsilon_{\mathrm{ES},yy,i}^n = \frac{p_i^n}{p_{\mathrm{BGK},yy,i}^n/Pr + (1-1/Pr)p_{yy,i}^n},$$

are the discrete values of the dimensionless coefficient $\varepsilon_{ij}RT$ of the ES-BGK model; see Eq. (7) in Section 2 for the definition in the continuous case. Above we have used the abbreviations $p_{\mathrm{BGK},xx,i}^n = \sum_{j=1}^J (C_{i,j_1}^n)^2 f_{\mathrm{BGK},i,j}^n \Delta\mathbf{c}$ and $p_{\mathrm{BGK},yy,i}^n = \sum_{j=1}^J (C_{i,j_2}^n)^2 f_{\mathrm{BGK},i,j}^n \Delta\mathbf{c}$, which are pressure tensor components computed from the reference distribution of the BGK model [6,23].

Expressions of the linearized reference distributions $F_{\mathrm{ref},i,j}^n$ and corresponding linear systems for other flow situations can be built following the same ideas [5,10].

It is difficult to estimate the values of the coefficients in the discrete reference distributions beforehand. Thus, in order to test the applicability of the suggested linearization of the reference function, we shall compare results obtained from the nonlinear and linear reference distributions.

We point out that the conservation laws are always fulfilled, since they are used to compute the coefficients. Therefore, this most important feature of Mieussens's original method is retained with the use of the linearization of the reference distribution. However, due to the linearization, the reference distribution does not strictly minimize entropy. More importantly, the approximation might lead to negative values of the reference distribution, similar to the Shakhov model and the Liu model for the collision term [5,10]. The H-theorem for the discrete transport equation will be valid only approximately, and a violation of the H-theorem will likely lead to instabilities in the numerical calculations. This might become an issue when only a small number of velocity nodes is used (so that the coefficients are not "small"). We shall come back to this point in the discussion of the results in Section 6.

Finally, we would like to say that if Mieussens's original DVM, instead of its linearization, is applied, our present method still would be useful. In particular it can be used to provide well-prepared initial data for the unknown coefficients $a_{\mathrm{BGK},i}^n$, $\Gamma_{\mathrm{BGK},i}^n$ and $\gamma_{\mathrm{BGK},i}^n$, through Eqs. (20), in the nonlinear system, which need be solved through the N–R algorithm.

5. Test examples

Shock waves. Shock waves are characterized by their upstream Mach number Ma, which is defined as

$$Ma = \frac{u_U}{a}, \tag{23}$$

where u_U and $a = \sqrt{5RT_U/3}$ are the flow and sound speed at the upstream equilibrium state.

In the numerical tests we consider a weak shock wave ($Ma = 1.5$), a medium shock wave ($Ma = 3.0$), and a strong shock wave ($Ma = 6.0$). For all tests, the gas molecules are modeled as ideal hard sphere molecules; the gas is

Table 1
Quantities used in the numerical tests of kinetic models for shock waves

Case	Domain width (m)	Mach number	Number of cells	Number of velocities	Bounds of velocities ($m\,s^{-1}$)	
					x direction	y (or z)
Sa	0.04	1.5	100	$12 \times 11 \times 11$	−2300, 3600	−2900, 2900
Sb	0.02	3.0	100	$18 \times 17 \times 17$	−3800, 5500	−4500, 4500
Sc	0.02	6.0	100	$32 \times 30 \times 30$	−7000, 10100	−8100, 8100
Sa2	0.04	1.5	200	$12 \times 11 \times 11$	−2300, 3600	−2900, 2900

Table 2
Quantities used in the numerical tests of kinetic models for planar Couette flow

Case	Kn	Domain width (mm)	Molecular model[a]	Speed of plate 2 ($m\,s^{-1}$)	Number of cells	Number of velocities	Bound of velocities ($m\,s^{-1}$)	
							y direction	x (or z)
Sa	0.025	353.3	HSM	300.0	100	$11 \times 10 \times 10$	−1100, 1400	−1100, 1100
Sb	0.025	353.3	MM	300.0	100	$11 \times 10 \times 10$	−1100, 1400	−1100, 1100
Sc	0.1	88.33	HSM	300.0	50	$11 \times 10 \times 10$	−1100, 1400	−1100, 1100
Sd	0.1	88.33	MM	300.0	50	$11 \times 10 \times 10$	−1100, 1400	−1100, 1100
Se	0.5	17.67	HSM	300.0	50	$11 \times 10 \times 10$	−1100, 1400	−1100, 1100
Sf	0.5	17.67	MM	300.0	50	$11 \times 10 \times 10$	−1100, 1300	−1100, 1100
Sg	1.0	8.833	HSM	300.0	25	$11 \times 10 \times 10$	−1100, 1300	−1100, 1100
Sh	1.0	8.833	MM	300.0	25	$11 \times 10 \times 10$	−1100, 1300	−1100, 1100
Si	0.5	17.67	HSM	600.0	50	$13 \times 12 \times 12$	−1100, 1700	−1300, 1300
Sj	0.5	17.67	HSM	1000.0	50	$16 \times 14 \times 14$	−1200, 2200	−1500, 1500
Sk	0.5	17.67	MM	600.0	50	$13 \times 12 \times 12$	−1100, 1700	−1300, 1300
Sl	0.5	17.67	MM	1000.0	50	$15 \times 14 \times 14$	−1200, 2200	−1600, 1600

[a] In the column of "Molecular model", "HSM" means hard sphere molecules, and "MM" means Maxwell molecules.

helium; the upstream temperature is 160.0 K; the upstream number density (defined as density over molecular mass) is $2.889 \times 10^{21}\ m^{-3}$; Boltzmann's constant is $k = 1.381 \times 10^{-23}\ J\,K^{-1}$; molecular mass of Helium $m = 6.65 \times 10^{-27}$ kg [24]. Grid size, number of nodes, etc. follow Mieussens's choice [5–10,23] and are given in Table 1.

The upstream mean free path l is 1.287 mm, based on the definition [1]

$$l = \mu \frac{\sqrt{RT}}{nkT}, \tag{24}$$

where $n = \rho/m$ is the number density, μ is the viscosity as computed from the empirical expression [1–4]

$$\mu(T) = \mu_0 \left(\frac{T}{T_0} \right)^{\omega}, \tag{25}$$

where μ_0 is the viscosity at the reference temperature T_0, and ω is a positive number of order 1, which is related to the power index γ in the inverse power potentials between particles [1–5],

$$\omega = \frac{\gamma + 3}{2(\gamma - 1)}. \tag{26}$$

The reference temperature is $T_0 = 273.0$ K which gives $\mu_0 = 1.86 \times 10^5\ kg\,m^{-1}\,s^{-1}$ [24].

Couette flow. The important parameter for planar Couette flow is the Knudsen number Kn, defined as the ratio of the mean free path l over the distance L between the two plates, $Kn = l/L$. In the tests of Couette flow Knudsen numbers $Kn = 0.025$, 0.1, 0.5 and 1.0 are used, with the two limiting situations for the molecular model, hard sphere molecules and Maxwell molecules. The relative plate speeds are set to be $300.0\ m\,s^{-1}$, $600.0\ m\,s^{-1}$ and $1000.0\ m\,s^{-1}$, corresponding to Mach numbers 0.975, 1.950 and 3.251. Altogether, there are twelve different test situations, see Table 2 for details, which shows the relevant quantities used in the numerical tests. For all numerical tests the material is argon, the temperature of both plates is 273.0 K; speed of plate 1 is zero; speed of plate 2 is chosen as indicated in Table 2; number density at initial state is $1.4 \times 10^{20}\ m^{-3}$; reference temperature is 273.0 K with $\mu_0 = 1.9552 \times 10^{-5}\ kg\,m^{-1}\,s^{-1}$ [25]; the molecular mass of argon is 6.63×10^{-26} kg [25,26]. The mean free path l from Eq. (24) is 8.833 mm for the initial state.

For each test case, the BGK model, the ES-BGK model with $b = -0.5$ ($Pr = 2/3$), the $\nu(C)$-BGK model [10], the $\nu(C)$-ES-BGK model with $b = -0.5$ ($Pr \cong 2/3$, see Table 2 in [10] for detail) have been computed.

6. Results and discussion

Due to space limitations, only a small part of the produced data and graphs can be shown. A wide array of results is presented in Ref. [5].

6.1. Preliminary comments

Since there is no fixed coordinate label for the shock profile inherent to the problem [3,9], all shock wave data is analyzed after shifting the curves such that in the origin, $x = 0$, of the new Cartesian frame the density takes on the arithmetic mean of the downstream and upstream values [3]. For planar Couette flow, no shifting is needed since the positions of the boundaries are fixed.

A good measure for the accuracy of the results obtained with the linearized reference distribution as compared to the nonlinear one is given by the relative error of the results for macroscopic quantities. Since the relative error will be meaningless when a quantity has values near to zero, we only consider average relative errors for density, velocity, temperature and pressure, but not for viscous stress or heat flux (which vanish in the equilibria upstream and downstream of shock waves and in the middle position of Couette flow).

For both, the original and the linearized reference distributions, the final computational results are converged for all tests (no changes when computational time was doubled), and the numerical method is stable (no unstable behavior observed).

In steady state, for shock waves the mass flux ρu_x, the momentum flux $\rho u_x^2 + p_{xx}$, and the energy flux $1.5 p u_x + 0.5\rho u_x^3 + p_{xx}u_x + q_x$ all should be constant in the whole domain [5]; while for planar Couette flow the quantities $u_x = 0$, p_{xx}, σ_{xy}, $u_y\sigma_{xy} + q_x$ should be constant in the whole domain [5]. These conditions were fulfilled in all computational results [5].

6.2. Effect of space and velocity grids

As pointed out in the Section 5, the choice of space and velocity grids follow Mieussens [6–9,23]. Their influence on results of macroscopic quantities have been discussed in detail elsewhere [5–10]. In [5], several choices of space and velocity grids have been applied and compared for the kinetic models with the linearized reference distribution f_{ref}. From that comparison, the space and velocity grids in Tables 1 and 2 are acceptable. Further increase of the number of position nodes, bounds of discrete velocities, and number of discrete velocities will only give less than 0.01 relative average error for density, velocity and temperature. Due to limited space, only one example is shown here: Fig. 1 shows the velocity profiles from the ES-BGK model with linearized f_{ref} for two different space grids (cases Sa and Sa2 of Table 1) at $Ma = 1.5$. The difference of two curves in Fig. 1 is not noticeable.

6.3. Comparison with original Mieussens's DVM

When the computational time for *each time step* is considered, using the linearized reference distribution f_{ref} can save 20∼40% of computational time compared to using the original distribution f_{ref} in each test case and any kinetic model. The difference between results using the linearized and the original reference distributions depends on the kinetic model and test case considered.

Generally the time saved in the ES-BGK model (∼30% for shock waves, ∼40% for Couette flow) is larger than the time saved in the BGK model (∼20% for shock waves, ∼30% for Couette flow), which reflects that in the ES-BGK model a nonlinear system of equations needs to be solved twice at each node [5,6], while only one nonlinear system must be solved for the BGK model.

The application of the linearized f_{ref} in the BGK model and the ES-BGK model does not introduce any noticeable errors in all tests, e.g. there are no visible differences in Fig. 2 which shows the density profiles from the BGK model at $Ma = 6.0$ and Fig. 3 which shows the density profiles from the ES-BGK model at $Ma = 3.0$.

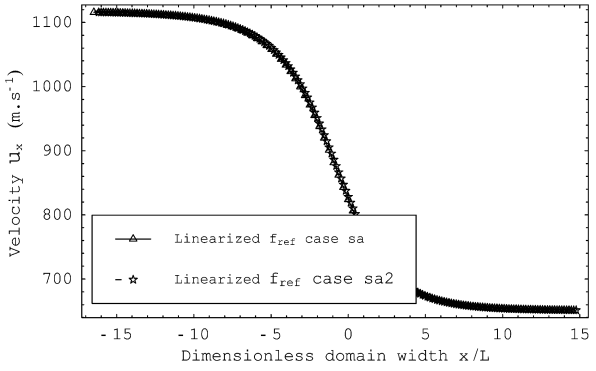

Fig. 1. Velocity profiles of shock waves with $Ma = 1.5$ from the ES-BGK model with linearized f_{ref} and two choices of space grid.

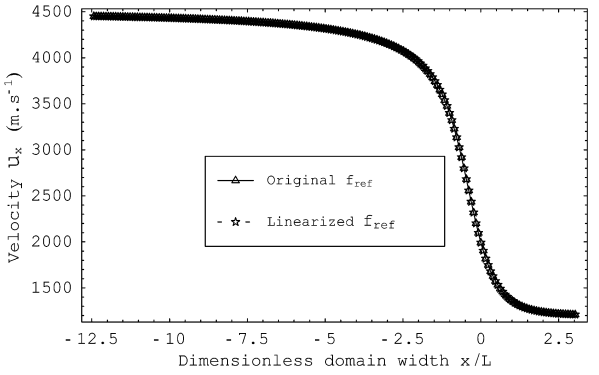

Fig. 2. Velocity profiles of shock waves with $Ma = 6.0$ from the BGK model.

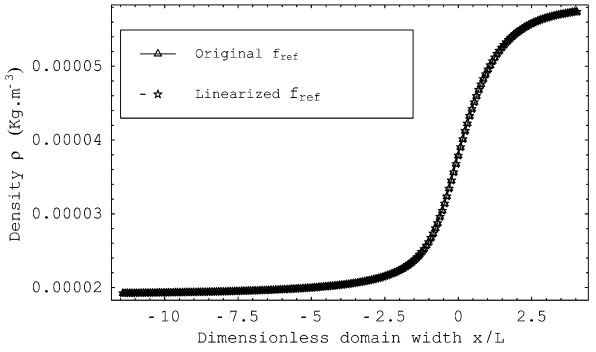

Fig. 3. Density profiles of shock waves with $Ma = 3.0$ from the ES-BGK model.

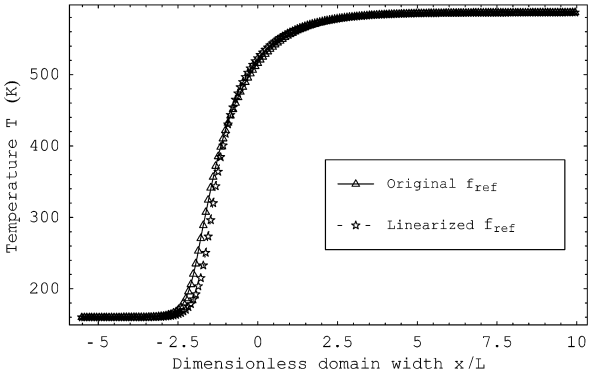

Fig. 4. Temperature profiles of shock waves with $Ma = 3.0$ from the $\nu(C)$-BGK model.

The application of the linearized reference distribution in the $\nu(C)$-BGK model works well for planar Couette flow, but not so good for shock waves at $Ma = 3.0$ and 6.0, in which cases the average relative errors are found to be 0.05 or higher. Fig. 4 shows the temperature profiles from the $\nu(C)$-BGK model using the linearized and using the original reference distribution at $Ma = 3.0$, in which the relative difference of the two curves in the middle part is as large as 0.20. Note, however, that this is due to the steepness of the curves where a small shift of the profile can result in a large change of the value observed at a location. Despite of this, the two curves give a reasonable optical fitness.

When the linearized distribution f_{ref} is applied in the $\nu(C)$-ES-BGK model, the results do not converge for $Ma = 6.0$, but are close to the results obtained using the original f_{ref} for other Mach numbers with average relative errors below 0.01. Fig. 5 shows the density profiles from the $\nu(C)$-ES-BGK model for case *Sc* in Table 2 ($Kn = 0.1$, 300.0 m s^{-1} plate speed, hard sphere molecules). Fig. 6 shows the temperature profiles from the $\nu(C)$-ES-BGK model for case Si in Table 2 ($Kn = 0.5$, 600.0 m s^{-1} plate speed, hard sphere molecules). The difference between using the linearized f_{ref} and using the original f_{ref} in Figs. 5 and 6 is invisible.

The results show that the linearization leads to problems particularly with those kinetic models where the collision frequency depends on velocity [9,10]. We offer the following explanation for this failure: The linearization involves the expansion of an exponential as $\exp(-\eta^2 - a\eta) \cong \exp(-\eta^2)(1 - a\eta)$. While the original expression is strictly nonnegative, the expanded function can become negative for larger values of $a\eta$. This leads to a negative reference distribution and in turn will lead to negative distribution functions. The Maxwellian $\exp(-\eta^2)$ suppresses these negative values quite effectively, so that this will happen only when the expansion coefficient a is rather large. However, in the $\nu(C)$-ES-BGK model and the $\nu(C)$-BGK model, the reference distribution is multiplied by the collision frequency

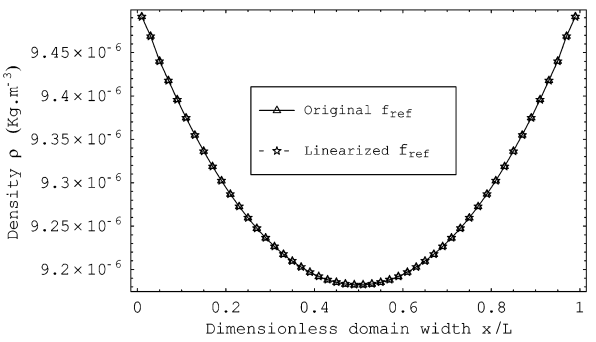

Fig. 5. Density profiles of planar Couette flow at situation Sc ($Kn = 0.1$, 300.0 m s^{-1} plate speed, hard sphere molecules) from the $\nu(C)$-ES-BGK model.

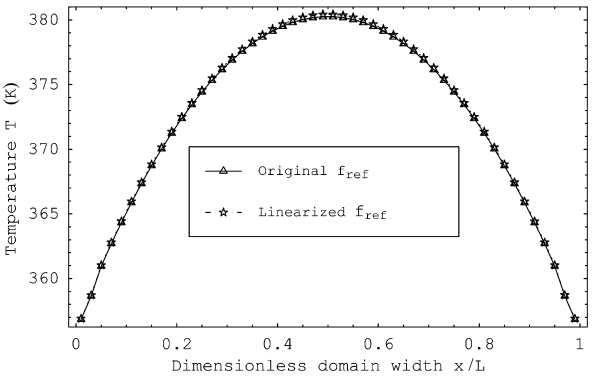

Fig. 6. Temperature profiles of planar Couette flow at situation Si ($Kn = 0.5$, 600.0 m s^{-1} plate speed, hard sphere molecules) from the $\nu(C)$-ES-BGK model.

ν which strongly increases with η. For example, the collision frequency for hard spheres is given by (erf(x) denotes the error function)

$$\nu_{\mathrm{HS}} = \nu_0(\rho, T)\left\{\exp\left(-\eta^2\right) + \frac{\sqrt{\pi}}{2}\left(\frac{1}{\eta} + 2\eta\right)\operatorname{erf}(\eta)\right\}. \tag{27}$$

Then, the Maxwellian is less effective in suppressing the negative values, which thus become significant already for smaller values of the expansion coefficient a. We believe that negative values of the distribution function are the cause for low quality results and instabilities. Also note that the negative values will occur and influence the results when the actual distribution is markedly different for the local Maxwellian, that is in case of strong non-equilibrium. This is the reason why problems arise for flows with large Mach numbers.

From the tests, we see that the applicability of our method is not dependent on molecule models (unless the collision frequency depends on velocity) and Knudsen number.

7. Conclusion

In this work, a modification of the original Mieussens's discrete velocity model is presented. The basic idea is to use a linearized expression, instead of a whole exact expression, of the reference distribution function f_{ref} in the numerical scheme. Results from this modified scheme are almost identical to results from the original scheme for most test cases, while up to 40 percent of computational time can be saved. The method works particularly well with the classical BGK and ES-BGK models, while it can be used in the corresponding models with velocity dependent collision frequency only for lower Mach numbers, or for very fine velocity meshes.

Acknowledgements

This research was supported by the Natural Sciences and Engineering Research Council (NSERC) of Canada. The authors wish to thank Dr. Luc Mieussens for many helpful discussions on his discrete velocity model. YZ would also like to thank Prof. Jason Reese in the University of Strathclyde and the Leverhulme Trust in the UK for current support that enabled him to write the paper.

References

[1] H. Struchtrup, Macroscopic Transport Equations for Rarefied Gas Flows—Approximation Methods in Kinetic Theory, Interaction of Mechanics and Mathematics Series, Springer, Heidelberg, 2005.
[2] M.N. Kogan, Rarefied Gas Dynamics, Plenum Press, 1969.
[3] C. Cercignani, Rarefied Gas Dynamics: From Basic Concepts to Actual Calculations, Cambridge University Press, 2000.
[4] V. Garzo, A. Santos, Kinetic Theory of Gases in Shear Flows, Kluwer Academic Publishers, Dordrecht, 2003.
[5] Y. Zheng, Analysis of kinetic models and macroscopic continuum equations for rarefied gas dynamics, Ph.D. thesis, Dept. Mech. Eng., Univ. of Victoria, Canada, 2004.

[6] L. Mieussens, Discrete-velocity models and numerical schemes for the Boltzmann-BGK equation in plane and axisymmetric geometries, J. Comput. Phys. 162 (2000) 429–466.
[7] L. Mieussens, Discrete velocity model and implicit scheme for the BGK equation of rarefied gas dynamics, Math. Models Methods Appl. Sci. 10 (2000) 1121–1149.
[8] L. Mieussens, Convergence of a discrete-velocity model for the Boltzmann-BGK equation, Comput. Math. Appl. 41 (2001) 83–96.
[9] L. Mieussens, H. Struchtrup, Numerical comparison of BGK-models with proper Prandtl number, Phys. Fluids 16 (2004) 2797–2813.
[10] Y. Zheng, H. Struchtrup, Ellipsoidal statistical BGK model with velocity-dependent collision frequency, Phys. Fluids 17 (2005) 127103 (1–17).
[11] P.L. Bhatnagar, E.P. Gross, M. Krook, A model for collision processes in gases. I: small amplitude processes in charged and neutral one-component systems, Phys. Rev. 94 (1954) 511–525.
[12] J. Lowell, H. Holway, New statistical models for kinetic theory: methods of construction, Phys. Fluids 9 (1966) 1658–1673.
[13] P. Andries, B. Perthame, The ES-BGK model equation with correct Prandtl number, in: AIP Conf. Proc., vol. 585, 2001, pp. 30–36.
[14] Y. Zheng, H. Struchtrup, Burnett equations for the ellipsoidal statistical BGK model, Continuum Mech. Thermodyn. 16 (2004) 97–108.
[15] H. Struchtrup, The BGK-model with velocity-dependent collision frequency, Continuum Mech. Thermodyn. 9 (1997) 23–31.
[16] F. Bouchut, B. Perthame, A BGK model for small Prandtl number in the Navier–Stokes approximation, J. Stat. Phys. 71 (1993) 191–207.
[17] L.B. Barichello, A.C.R. Bartz, M. Camargo, C.E. Siewert, The temperature-jump problem for a variable collision frequency model, Phys. Fluids 14 (2002) 382–391.
[18] C. Cercignani, The method of elementary solutions for kinetic models with velocity-dependent collision frequency, Ann. Phys. 40 (1966) 469–481.
[19] C. Cercignani, Knudsen layers: theory and experiment, in: U. Muller, K.G. Rosner, B. Schmidt (Eds.), Recent Developments in Theoretical and Experimental Fluid Mechanics, Springer-Verlag, Berlin, 1979, pp. 187–195.
[20] H.C. Yee, Construction of explicit and implicit symmetric TVD schemes and their applications, J. Comput. Phys. 68 (1987) 151–179.
[21] W.H. Press, B.P. Flannery, S.A. Teukolsky, W.T. Vetterling, Numerical Recipes, Cambridge University Press, 1986.
[22] J.E. Dennis, R.B. Schnabel, Numerical Methods for Unconstrained Optimization and Nonlinear Equations, Prentice-Hall, 1983.
[23] L. Mieussens (Toulouse, France), private communication, 2003.
[24] G.C. Pham-Van-Diep, D.A. Erwin, E.P. Muntz, Testing continuum descriptions of low-Mach-number shock structures, J. Fluid Mech. 232 (1991) 403–413.
[25] A. Schuetze, Direct simulation by Monte Carlo modeling Couette flow using dsmc1as.f: A user's manual, Technical Report, Dept. Mech. Eng., Univ. of Victoria, Canada, 2003.
[26] R.B. Bird, W.E. Stewart, E.N. Lightfoot, Transport Phenomena, second ed., John Wiley & Sons, 2002.